Effect of fin efficiency models on air-side performance of crimped spiral fin-and-tube heat exchangers

Parinya Kiatpachai[a], Anotai Suksangpanomrung[a], Phubate Thiangtham[b], Chanyoot Keepaiboon[b], Weerapun Duangthongsuk[c], Somchai Wongwises[d*]

[a]Department of Mechanical Engineering, Academic Division, Chulachomklao Royal Military Academy, Nakhon Nayok 26001, Thailand

[b]Thai-Ingenieur Co., Ltd, Bangkok, 10510, Thailand

[c]Department of Mechanical Engineering, Southeast Asia University, Bangkok, Thailand

[d]Fluid Mechanics, Thermal Engineering and Multiphase Flow Research Lab. (FUTURE), Department of Mechanical Engineering, Faculty of Engineering, King Mongkut's University of Technology Thonburi, Bangmod, Bangkok 10140, Thailand

*Corresponding author: somchai.won@kmutt.ac.th

Abstract In this study, we investigate the effect of fin efficiency (η_f) models on the airside performance (ASPs) of crimped, spiral fin and tube heat exchangers (SHXs). The analysis of ASP is calculated using different fin efficiency models based on the assumptions of constant heat flux for each Reynolds number, constant heat transfer area with negligible fin thickness, and constant fin geometry for four exanimate heat exchangers (HX). The L-Rectangular, L-Convex, L-Triangular, and L-Concave models of longitudinal fin efficiency are used in the calculation and compared with the R-Rectangular model for radial fin efficiency that looks more realistic than the tested crimped spiral fin. The four samples are the crimped SHX. The well-insulated, open wind tunnel is used for heat transfer between two working fluids, i.e., ambient air and hot water. The experiment is carried out over a range of V_{fr} (1-6 m/s) or Re_{do} of 3,000 to 12,000. The results show that the L-Triangular, L-Convex, and L-Rectangular models for fin efficiency provide trends of heat transfer coefficients that are more similar to the realistic R-Rectangular model. However, we found another model over-predicting the heat transfer coefficient by as much as 5-10%. This model uses the L-Concave model of fin efficiency with various Cu and Al fins, each with 3 or 4 tube rows. Moreover, we demonstrate a similar trend and value for fin efficiency between L-Triangular and R-Rectangular models. The effect of fin efficiency models and fin materials has a strong variation in terms of fin efficiency. In contrast, the number of tube rows, whether 3 or 4, has no significant effect on fin efficiency. This proposed research can be generally applied to selection of a model by fin efficiency and prediction of safety factors in designing crimped SHX.

Keywords**:** tube, heat transfer, fin efficiency, heat exchanger, number of tube row

1. Introduction

Extended surfaces are generally used in heat transfer enhancement techniques and energy technologies. The most favorable application that uses the theory of extended surface area is the fin-and-tube heat exchanger. A heat exchanger (HX) is a thermal medium for transfer of heat from one fluid (air) to another (water) through a wall. The extended wall surface area is dominant in the heat transfer rate. Moreover, the heat transfer rate is directly proportional only to the heat transfer coefficient and the temperature differences between both fluids. Therefore, if fins are attached to the wall surface on the air side of the HX, the total heat transfer is increased because of the extended fin surface area. Moreover, there are many types of fin geometry including plate fins and spiral fins. Each of these has a dissimilar fin efficiency providing different ASP of HX in terms of the heat transfer rate. There are scientists who have studied heat transfer performance with different fin geometries, including compounded-fin, louvered-fin, wavy-fin, plain-fin, and other variations. These valuable studies on plate fin-and-tube HX are published as general information in the research, as detailed in the publication.

We found in our investigation that there are many works on plate fin-and-tube HX. However, there are fewer studies on the spiral fin-and-tube HX [1-13], as follows:

Naphan and Wongwises [1] and Wongwises and Naphon [2,3] investigated theoretically and experimentally the airside performance of a spirally finned tube HX operating in dehumidifying, dry-surface, and wet-surface conditions. Moreover, they tested HXs employing crimped, spiral-finned tubes.

Nuntaphan et al. [4,5] investigated the influence of the tubes' outside diameter, fin pitch, transverse tube pitch, and tube layout. Furthermore, they proposed correlations for crimped SHX under dehumidification and drying processes. They proposed correlations of heat transfer coefficients in the case of a low Reynolds number. Moreover, Pongsoi et al. [6] reported heat transfer performances and friction characteristics for spiral fin and tube HX. A literature survey also reveals that research groups have studied spiral fin and tube HX extensively [7-13]. They studied the ASP of crimped spiral fins [7-9], L-footed spiral fins [10-12], and serrated welded spiral fins [13]. In addition, the j-Colburn factor and f-friction factor correlations are proposed for HX design.

However, fin efficiency models can be used to predict the ASP of spiral fin-and-tube HX. For some published works, data reduction is performed by using the same type of fin efficiency model, even if they were studied for different fin types. This leads to the interesting topic of what a suitable model for fin efficiency should be for predicting heat transfer. Mokheimer [14] studied the performance of annular fins with different profiles. Mokheimer also reported the effect of variable ho on the performance of an extended surface [15]. The crimped spiral- finned tube HX is another type for industrial application in waste-heat recovery. The fin base in a sine shape provides a larger surface contact area with the outside tube surface. The crimped spiral fin gives a greater than London area

goodness when compared with the circular fin [16] and the plain fin [17,18], which is presented in a ratio of desired output to required input, as illustrated in Fig.1

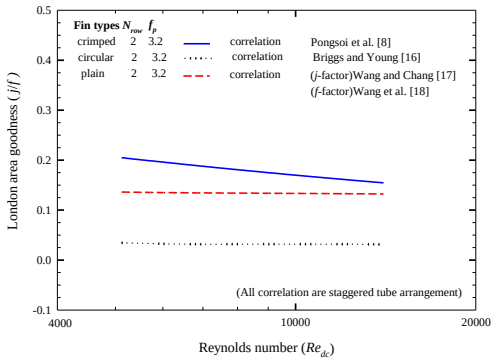

Fig.1 Comparison of London area goodness in various fin types

The longitudinal model of fin efficiency is used to perform data reduction for a general kind of fin for the air-side heat transfer performance of a finned tube HX, which is uncertain in a different shape on realistic HX design.

In order to clarify the effect of the shape in a variation of the fin efficiency model on HX design for a crimped spiral fin, this study therefore presents the effect of fin efficiency models on the airside heat transfer performance of crimped, spiral fin-and-tube HX based on the assumptions of the heat flux constant for each Reynolds number, with a heat transfer area fixed with negligible effect on fin thickness and fin geometry for four exanimate HXs.

Moreover, this study presents the effect of fin material and the number of tube rows in a variation of copper fins and aluminum fins with 3 or 4 rows of crimped spiral fin and tube HX having a copper tube, an outside diameter of 16.35 mm, and a transverse tube pitch of 35 mm. The comparison between the radial model for fin efficiency and other models presents a challenge in suitably and comfortably predicting the ASP of a crimped, spiral fin-and-tube HX. Finding the optimal fin efficiency model would be useful in HX applications for waste-heat

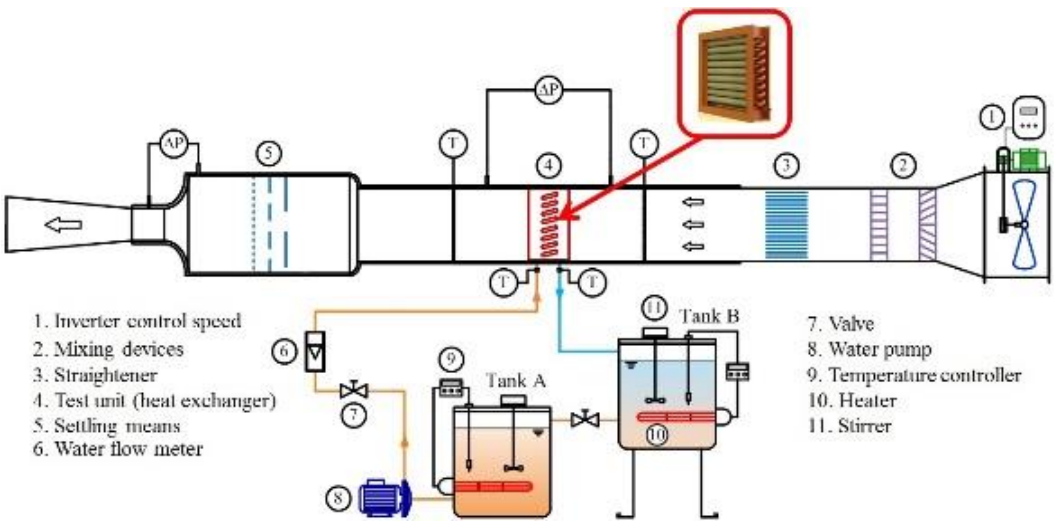

Fig.2 Schematic diagram of the experimental apparatus [From Pongsoi et al. [9], with permission from Elsevier]

2. Experimental Apparatus

The apparatus is illustrated in Fig.2 Air and water are the working fluids for the air supply system and the hot water flow loop. The instrumentation systems are used in the system.

We investigate copper and aluminum crimped SHXs with varying numbers of tube rows (3 and 4 rows). The waterside circuit and dimensions of the crimped spiral fin and tube HXs are shown in Fig.3

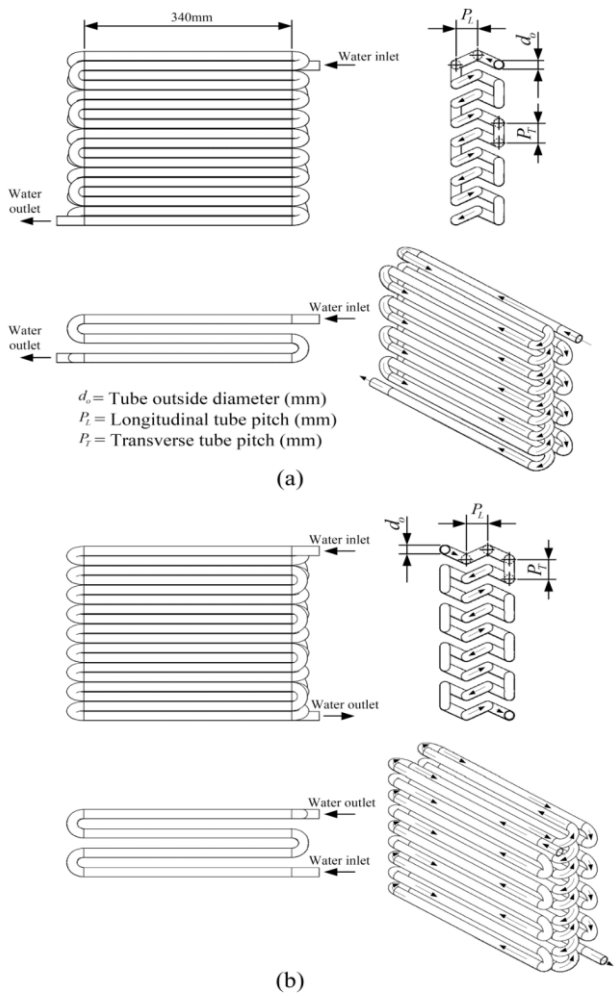

Fig.3 Geometric details of water flow circuit and tube arrangement of the HX for (a) N_{row}=3 and (b) N_{row}=4 [10]

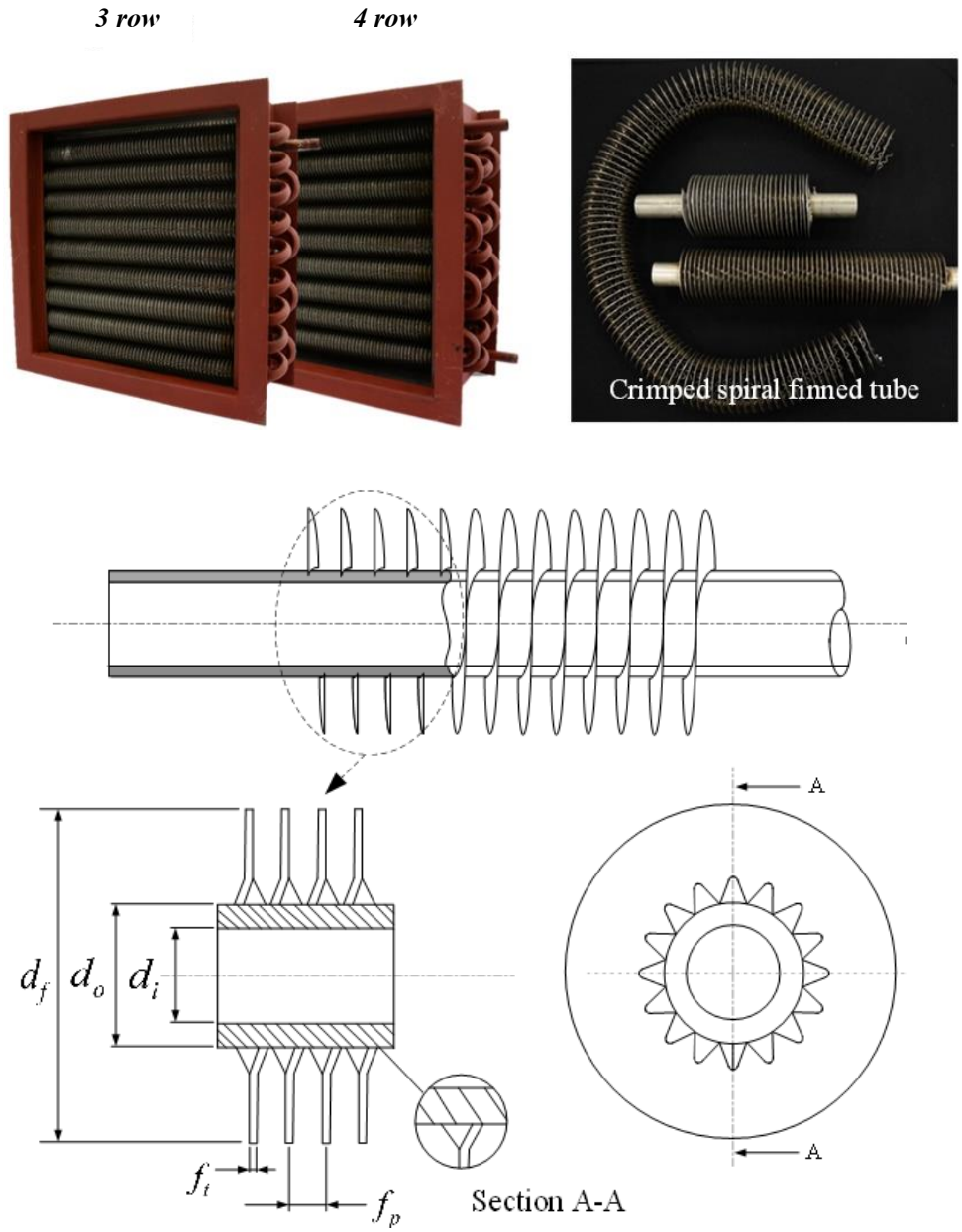

Fig.4 Geometric details and photos of the tested crimped spiral fin and tube heat exchangers

[From Pongsoi et al. [7], with permission from Elsevier]

Table1. Detailed geometric parameters of the test samples (Crimped spiral fin)

No.	d_f (mm)	d_i (mm)	d_o (mm)	f_p (mm)	f_t (mm)	P_L (mm)	P_T (mm)	Fin material	N_{row}
1	35	13.5	16.35	6.3	0.5	35	35	Cu	3
2	35	13.5	16.35	6.3	0.5	35	35	Cu	4
3	35	13.5	16.35	6.3	0.5	35	35	Al	3
4	35	13.5	16.35	6.3	0.5	35	35	Al	4

Notes: (Cu=copper, Al=aluminium)

Table.2 Experimental conditions

Inlet-air-dry bulb temperature, ^oC	31.5±0.5
Inlet-air frontal velocity, m/s	1-6 or Re_{do} (3000-1200)
Inlet-water temperature, ^oC	50-70
Water flow rate, LPM	10-14

The details of the crimped spiral finned tube are indicated in Fig.4 Moreover, Table.1 presents the geometric parameters of the test sections.

The open-type wind tunnel generates air cross flow through the test sections (crimped SHXs). Heat is transferred from the hot water flowing through the HX to the air. The steel plate in a cross sectional area of 0.43 x 0.48 m is built as a wind tunnel structure. The air duct is covered by insulation on the exterior wall surface with a 16 mm thick insulation sheet. The ambient air flows through the mixing device, the straightener, and the test section, blown by an axial flow fan at 2.2 kW. The speed of airflow can be controlled using an inverter. Temperatures at various locations are measured by thermocouple probes (T-type copper-constantan). The ASHRAE standard is used for locating the position of the thermocouple. Data collection, including inlet and outlet temperatures, is measured and recorded continuously. All measuring devices are calibrated. A digital manometer measures air pressure drops between the test section inlet and outlet and venturi. The details of measurement and experiment can be seen in [10].

Fig.2 demonstrates the hot-water flow loop, which consists of two tanks, a heater, a water pump, and a flow meter. The purpose of the hot water flow loop is to transfer heat to the air. For all experimental conditions, the water temperature and flow rate are maintained while the airflow is increased to a high Reynolds number.

Table.3 The accuracy of the measurement

Parameters	Accuracy
Inlet-air dry-bulb temperature, ^{o}C	±0.1
Pressure drop, Pa	±0.5% of full scale
Inlet-water temperature, ^{o}C	±0.1
Water flow rate, LPM	±0.02 of full scale

Table.4 Uncertainties of the derived experimental values

Parameters	Uncertainties (%)
Air –side heat transfer, Q_a	±2.12
Water-side heat transfer rate, Q_w	±3.37
Frontal velocity, V_{fr}	±0.46
Reynolds number, Re_{do}	±0.34
Air-side heat transfer coefficient, h_o	±4.02
Colburn factor, j	±4.04

The experimental data are recorded, and when the system is in a steady state, it can be confirmed as a data point in determining the experiment. The tested experiment conditions are illustrated in Table. 2 , and tables 3 and 4 show the accuracies of the measurement uncertainties.

3. Data Reduction

The NTU method and total thermal resistance are used in the data reduction for the UA product, which can be represented as follows:

The Q_a is given as:

$$Q_a = m_a c_{P,a} \Delta T_a \quad (1)$$

The Q_w *i*s given as:

$$Q_w = m_w c_{P,w} \Delta T_w \quad (2)$$

The Q_{ave} is given as:

$$Q_{ave} = \frac{Q_a + Q_w}{2} \quad (3)$$

Total thermal resistance is used in data reduction for the UA product and heat transfer coefficient as follows:

$$\frac{1}{UA}=\frac{1}{h_i A_i}+\frac{\ln(d_o/d_i)}{2\pi k_t L}+\frac{1}{\eta_o h_o A_o} \tag{4}$$

Equations (5) - (9) for one fluid mixed and one fluid unmixed are used to determine the h_o as follows:

For multipass parallel cross-flow with N_{row}= 3 and 4:

(N_{row} = 3),

$$\varepsilon_P=1-\left(1-\frac{K}{2}\right)^2 e^{-3K/C_A^*}-K\left[1-\frac{K}{4}+\frac{K}{C_A^*}\left(1-\frac{K}{2}\right)\right]e^{-K/C_A^*},K=1-e^{-NTU_A(C_A^*/3)} \tag{5}$$

(N_{row} = 4),

$$\varepsilon_P=1-\frac{K}{2}\left(1-\frac{K}{2}+\frac{K^2}{4}\right)-K\left(1-\frac{K}{2}\right)\left(1+2\frac{K}{C_A^*}\left[1-\frac{K}{2}\right]\right)e^{-2K/C_A^*}-\left(1-\frac{K}{2}\right)^3 e^{-4K/C_A^*},K=1-e^{-NTU_A(C_A^*/4)} \tag{6}$$

For multipass counter cross-flow with N_{row}= 3 and 4:

(N_{row} = 3),

$$\varepsilon_c=1-\left\{\left(1-\frac{K}{2}\right)^2 e^{3K/C_A^*}+\left[K\left(1-\frac{K}{4}\right)-\left(1-\frac{K}{2}\right)\frac{K^2}{C_A^*}\right]e^{K/C_A^*}\right\}^{-1},K=1-e^{-NTU_A(C_A^*/3)} \tag{7}$$

(N_{row} = 4),

$$\varepsilon_c=1-\left\{\frac{K}{2}\left(1-\frac{K}{2}+\frac{K^2}{4}\right)+K\left(1-\frac{K}{2}\right)\left[1-2\frac{K}{C_A^*}\left(1-\frac{K}{2}\right)\right]e^{2K/C_A^*}+\left(1-\frac{K}{2}\right)^3 e^{4K/C_A^*}\right\}^{-1},K=1-e^{-NTU_A(C_A^*/4)} \tag{8}$$

Where $C^* = C_{min}/C_{max}$ is equal to

$$\varepsilon_{pc}=\frac{\varepsilon_P+\varepsilon_C}{2} \quad \text{for } N_{row}=3 \text{ and } 4 \tag{9}$$

Where

$$\varepsilon=\frac{Q_{ave}}{Q_{\max}} \tag{10}$$

The Q_{max} can be expressed as:

$$Q_{\max}=(mc_P)_c(T_{h1}-T_{c1}) \text{ if } C_c<C_h \tag{11}$$

or

$$Q_{\max}=(mc_P)_h(T_{h1}-T_{c1}) \text{ if } C_h<C_c \tag{12}$$

where the UA can be defined from

$$NTU=\frac{UA}{C_{\min}} \tag{13}$$

so that

$$UA=C_{\min}(NTU) \tag{14}$$

The in-tube heat transfer coefficient is defined from Gnielinski's correlation [19]:

$$h_i=\left(\frac{k_w}{d_i}\right)\frac{(\mathrm{Re}_{di}-1000)\mathrm{Pr}(f_i/2)}{1+12.7\sqrt{f_i/2}\left(\mathrm{Pr}^{2/3}-1\right)} \tag{15}$$

where the friction factor is given by:

$$f_i=(1.58\ln \mathrm{Re}_{di}-3.28)^{-2} \tag{16}$$

where

$$\mathrm{Re}_{di}=\rho V d_i/\mu$$

The η_o is given as:

$$\eta_o=1-\frac{A_f}{A_o}(1-\eta) \tag{17}$$

where A_o is the total surface area.

The longitudinal fins and radial fin efficiency of the rectangular profile as shown in Figure 5(a-e) is reported by Gardner [20]:

Longitudinal fin of Rectangular profile (L-Rectangular)

$$\eta = \frac{\tanh mb}{mb} \tag{18}$$

Longitudinal fin of Convex parabolic profile (L-Convex)

$$\eta = \frac{1}{mb}\left[\frac{I_{2/3}(\frac{4}{3}mb)}{I_{-1/3}(\frac{4}{3}mb)}\right] \tag{19}$$

Longitudinal fin of Triangular profile (L-Triangular)

$$\eta = \frac{I_1(2mb)}{(mb)I_0(2mb)} \tag{20}$$

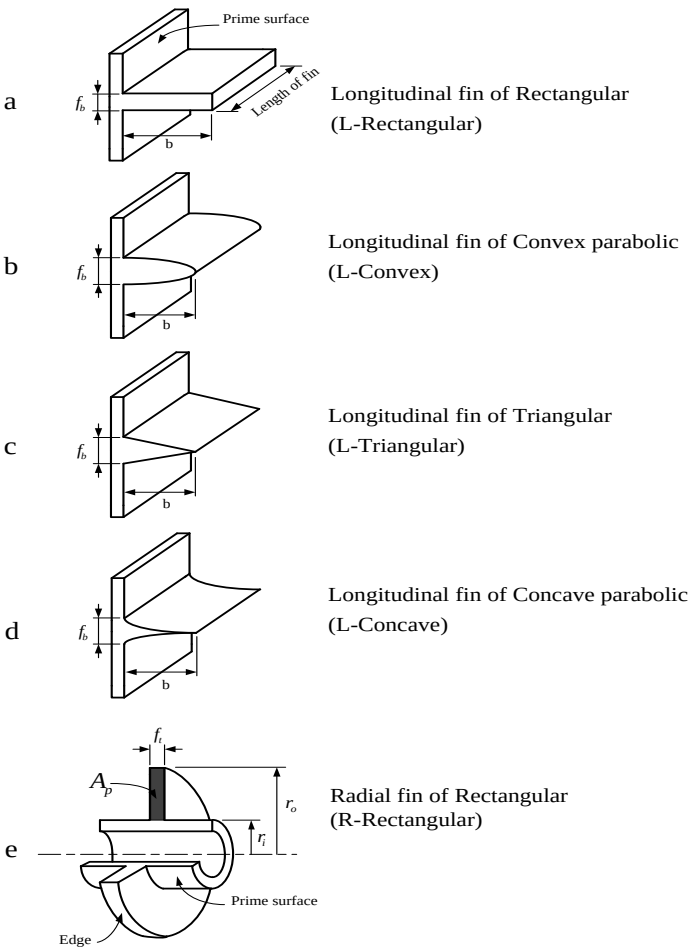

Fig.5 The patterns of the fin efficiency models. (a) L-Rectangular, (b) L-Convex, (c) L-Triangular, (d) L-Concave, (e) R-Rectangular [20]

Longitudinal fin of Concave parabolic profile (L-Concave)

$$\eta = \frac{2}{1+\sqrt{1+(2mb)^2}} \tag{21}$$

and radial fin of rectangular profile (R- Rectangular)

$$\eta = \frac{2\psi}{\phi(1+\psi)} \frac{I_1(\phi R_o)K_1(\phi R_i) - I_1(\phi R_i)K_1(\phi R_o)}{I_0(\phi R_i)K_1(\phi R_o) + I_1(\phi R_o)K_0(\phi R_i)} \tag{22}$$

where m is the fin performance factor

$$m = (\frac{2h_o}{k_f f_b})^{1/2} \tag{23}$$

and the terms of ϕ

$$\phi = (r_o - r_i)^{3/2}(\frac{2h_o}{k_f A_p})^{1/2} \tag{24}$$

where A_p is the area in profile of the fin, as shown in Figure 4(e):

$$A_p = f_t(r_o - r_i) \tag{25}$$

and the parameters R_o, R_i are function of the radius ratio (ψ) :

$$R_o = \frac{1}{1-\psi} \tag{26}$$

and

$$R_i = \frac{\psi}{1-\psi} \tag{27}$$

Where

$$\psi = \frac{r_i}{r_o} \tag{28}$$

The Colburn j factor is presented for the heat transfer performance of forced convection:

$$j = \frac{Nu}{\mathrm{Re}_{do}\,\mathrm{Pr}^{1/3}} = \frac{h_o}{\rho_a V_{\max} c_P}(\mathrm{Pr})^{2/3} \tag{29}$$

The fanning friction factor is dimensionless, related to entrance and exit pressure losses [21].

$$f = \left(\frac{A_{\min}}{A_o}\right)\left(\frac{\rho_m}{\rho_1}\right)\left[\frac{2\Delta P \rho_1}{G_c^2} - \left(1+\sigma^2\right)\left(\frac{\rho_1}{\rho_2}-1\right)\right] \tag{30}$$

4. Results and Discussion

In this part, the results are presented based on relative errors of approximately 5%.

In this study, the analysis of ASP is calculated using different fin efficiency models based on the assumptions of constant heat flux for each Reynolds number, a constant heat transfer area with negligible fin thickness, and a constant fin geometry for four exanimate HXs. L-Rectangular, L-Convex, L-Triangular, and L-Concave models of longitudinal fin efficiency are calculated and compared with the R-Rectangular model of radial fin efficiency that looks more realistic to the tested crimped spiral fin.

The effect of various fin efficiency models is studied and calculated for both Cu and Al fin materials with rows of 3 or 4 tubes. As shown in Figures 6-9, we observe an ho increase with increasing frontal air velocity over the range of examined frontal air velocity. In Figure 6-9, the use of L-Triangular, L-Convex, and L-Rectangular models of fin efficiency gives a heat

transfer coefficient that is more similar to the realistic R-Rectangular model.

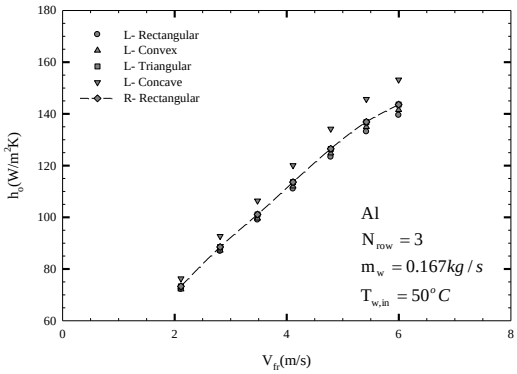

Fig.6 The effect of the fin efficiency model on h_o at $T_{w,in}$=50 ^{o}C and $m_{w,in}$=0.167 kg/s (aluminium fin)

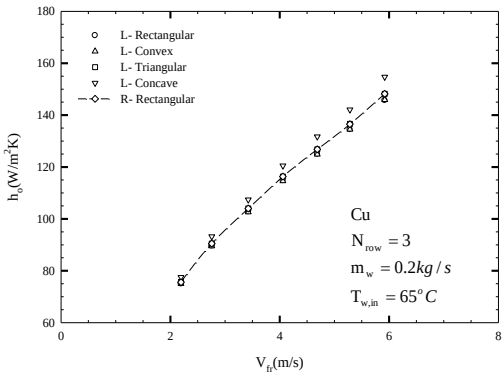

Fig.7 The effect of the fin efficiency model on h_o at $T_{w,in}$=65 ^{o}C and $m_{w,in}$=0.2 kg/s (copper fin)

However, it can be noted that the L-Concave model provides an over-prediction of the Colburn factor (j) and an ho of up to 5% (for the copper fin and 3-4 rows) and up to 10% (for the aluminum fin and 3-4 rows) when compared with the R-Rectangular model.

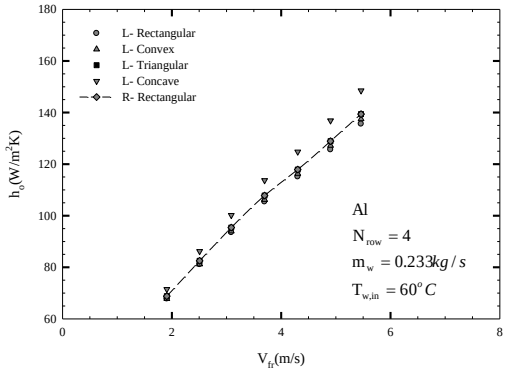

Fig.8 The effect of the fin efficiency model on h_o at $T_{w,in}$=60 ^{o}C and $m_{w,in}$=0.233 kg/s (aluminium fin)

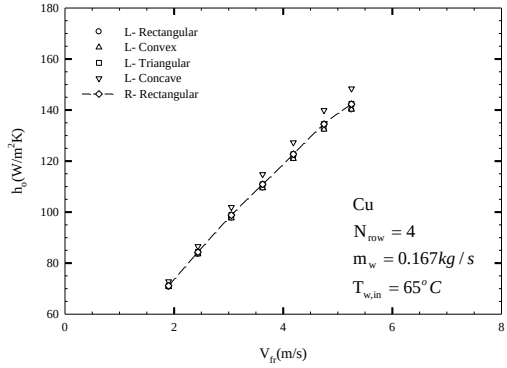

Fig.9 The effect of the fin efficiency model on h_o at $T_{w,in}$=65 ^{o}C and $m_{w,in}$=0.167 kg/s (copper fin)

In figures 10-13, we observe that the Colburn factor decreases with increasing Re_{do} over the examined range of the Re_{do}, which shows the effects of various fin efficiency models on the Colburn factor (j) for both Cu and Al fin materials with 3 and 4 tube rows giving the same result to Fig. 6-9

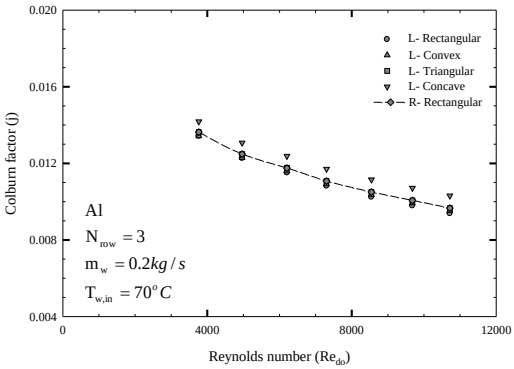

Fig.10 The effect of the fin efficiency model on the j factor at $T_{w,in}$=70 ^oC and $m_{w,in}$=0.2 kg/s (Aluminium fin)

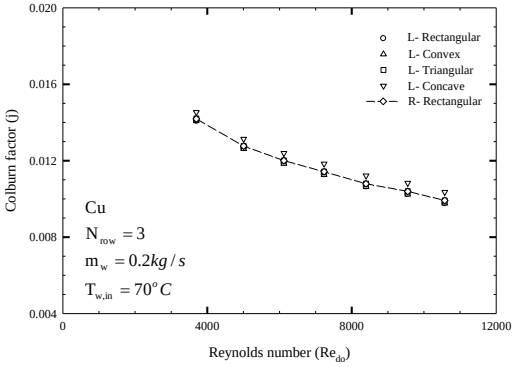

Fig.11 The effect of the fin efficiency model on the j factor at $T_{w,in}$=70 ^oC and $m_{w,in}$=0.2 kg/s (copper fin)

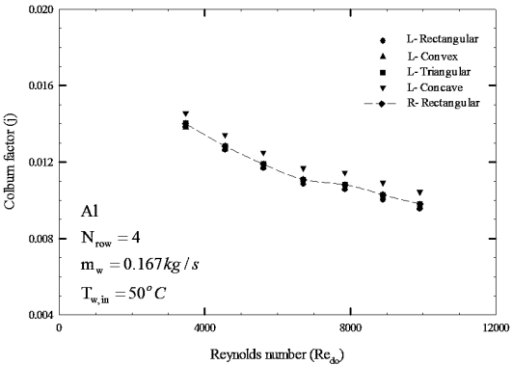

Fig.12 The effect of the fin efficiency model on the j factor at $T_{w,in}$=50 ^oC and $m_{w,in}$=0.167 kg/s (aluminium fin)

As shown in fig. 14-17, the relationship between fin efficiency and the Reynolds number is compared for Cu and Al materials with 3 to 4 tube rows. It obviously seems that fin efficiency decreases with increasing Redo. The surface temperature of a fin decreases more than the fin's base temperature and is negatively correlated with fin efficiency. Moreover, as the Re_{do} increases, downstream turbulence increases, which causes airflow mixing to increase.

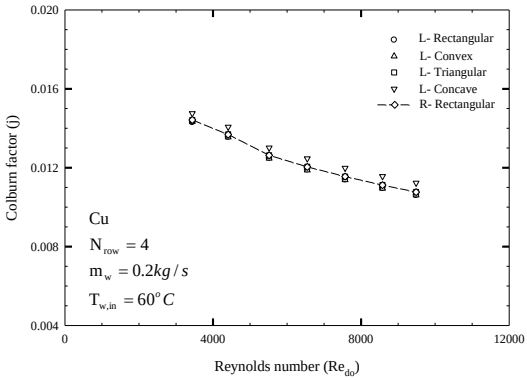

Fig.13 The effect of the fin efficiency model on the j factor at $T_{w,in}$=60 ^oC and $m_{w,in}$=0.2 kg/s (copper fin)

Fig.14 and 15 show the effect of the fin material on η_f . For the same model, the Cu material gives a higher fin efficiency than the Al material. In addition, the L-Rectangular model gives no significant difference in the value of fin efficiency compared to the L-Convex model over the range of tested Reynolds numbers for the Cu material. In contrast, for the Al material, the apparent differentiation between the L-Rectangular and L-Convex model is founded. Moreover, the results also show an interesting fact about the similarity of fin

efficiency between the L-Triangular and R-rectangular models.

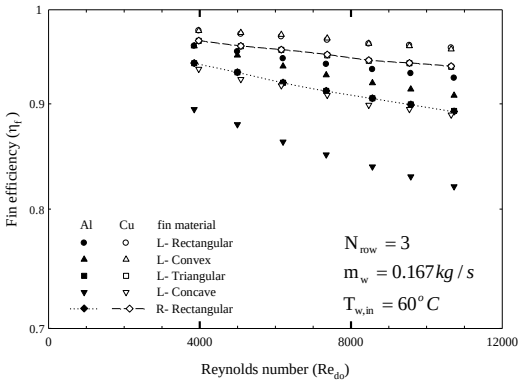

Fig.14 The effect of the fin efficiency model on fin efficiency at $T_{w,in}$=60 ^{o}C and $m_{w,in}$=0.167 kg/s (N_{row}=3)

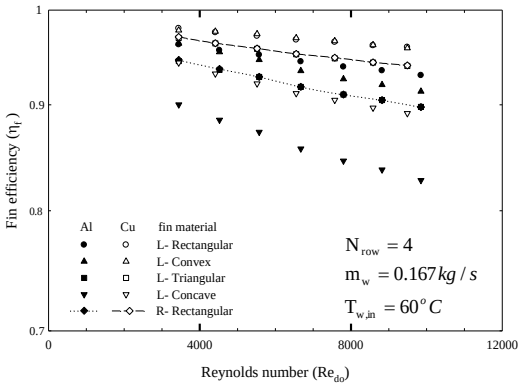

Fig.15 The effect of the fin efficiency model on fin efficiency at $T_{w,in}$=60 ^{o}C and $m_{w,in}$=0.167 kg/s. (N_{row}=4)

Fig. 16 and 17 show the effect of N_{row} on fin efficiency over the range of tested Reynolds numbers. The results show that the number of tube rows has no effect on fin efficiency. According to the results, the given constant heat flux for each Reynolds number leads to an inverse function between the heat transfer coefficient and fin efficiency.

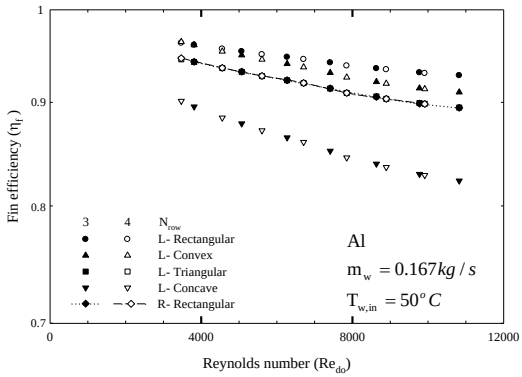

Fig.16 The effect of the fin efficiency model on fin efficiency at $T_{w,in}$=50 ^{o}C and $m_{w,in}$=0.167 kg/s (aluminium fin)

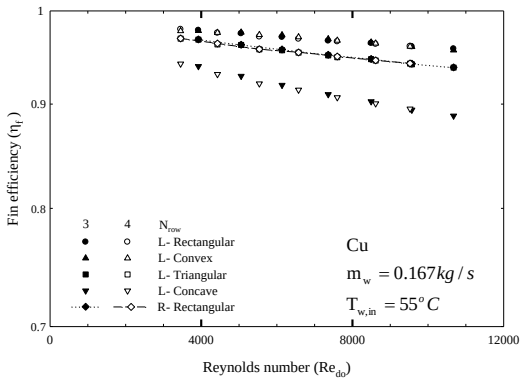

Fig.17 The effect of the fin efficiency model on fin efficiency at $T_{w,in}$=55 ^{o}C and $m_{w,in}$=0.167 kg/s (copper fin)

The L-Triangular model seems to be the suitable model for calculating fin efficiency when studying the crimped spiral fin. In addition, the L-Convex and L-Rectangular models can also be used to calculate the fin efficiency of the crimped spiral fin with insignificant results. On the other hand, the L-Concave model is not recommended because of the over-prediction of the calculation, leading to an error of 4-9% when compared with the R-

rectangular model. The L-Concave model provides the highest heat transfer coefficient due to the lowest η_f because the η_f is dependent on the extended surface area, which seems to be the lowest in the case of L-Concave model.

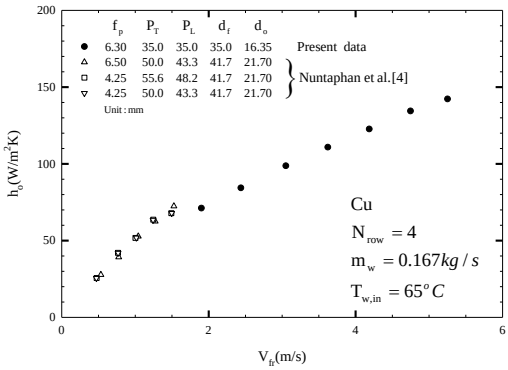

Fig.18 A comparison of h_o between the measured data and the experimental data of Nuntaphan et al. [4] (using the R-Rectangular model)

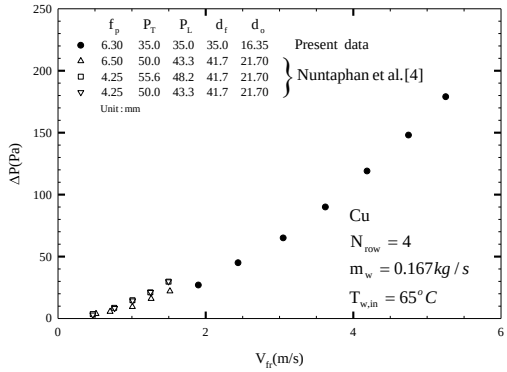

Fig.19 A comparison of pressure drop between the measured data and the data of Nuntaphan et al. [4] (using R-Rectangular model)

In addition, according to Fig. 18 and 19, the results show the connecting trend for h_o and the pressure drop of Nuntaphan et al. [4] at low Re_{do}, which is confirmed in the data presented in this research.

Calculation Flowchart

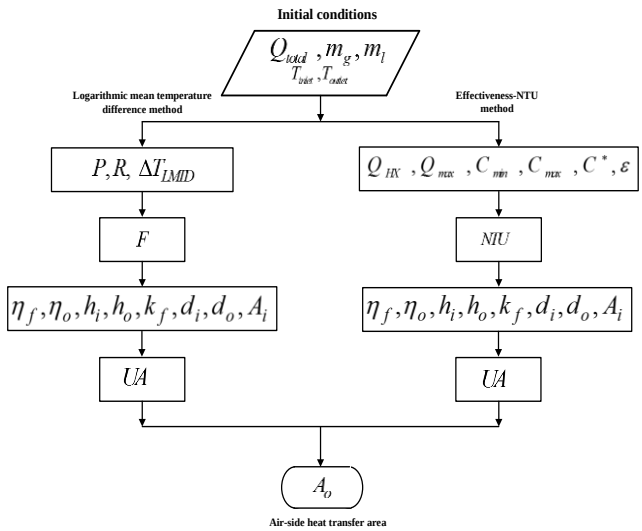

Fig.20 The calculation flowchart for the heat transfer area of the HX

Finally, for another error in HX design, the LMTD-NTU method (i.e., figure 20) does not provide exactly the same value because the LMTD method assumes an energy balance for Q, leading to an error of up to 25% in determining the heat transfer area, as reported by Park [22]. The reduction of data in finding the heat transfer area can be concluded from these methods. However, one can also use an assumption to reduce the complex equation in the calculation process by selecting a convenient equation such as the L-Triangular model instead of the R-Rectangular model in the term of η_f

5. Conclusion

This study presents the effect of η_f models on the ASP of crimped SHXs with a high Reynolds number (Re_{do}) of 3,000-12,000. The following conclusions were obtained:

- There are no significant differences for comparison of the Colburn factor (j) with respect to the η_f of the R-Rectangular model at the same conditions for the fin efficiency of the L-Rectangular, L-Convex, and L-Triangular models. However, using the L-Concave model for calculating the η_f gives over-predictions of up to 5% for the copper fin and 10% for the aluminum fin compared to the realistic R-Rectangular model.
- The η_f decreases as the Re_{do} increases under the same experimental conditions. The number of tube rows, whether 3 or 4 rows, has no significant effect on the η_f
- Among η_f models, the L-Triangular and R-rectangular models show similar trends for predicting heat transfer performance.
- For the effect of fin materials, the thermal conductivity of aluminum has a strong effect on the different values of fin efficiency between the L-Rectangular and L-Convex model. In contrast, there is no significant effect on the copper fin.
- Finally, this work proposes a convenient equation-the L-Triangular model-and heat transfer coefficient variation for the η_f models instead of the R-Rectangular model, which is a complex equation (i.e., Bessel Function) for SHX design.

Acknowledgments

The authors would like to thank Department of Mechanical Engineering, Academic Division, Chulachomklao Royal Military Academy (CRMA) and the Department of Mechanical Engineering, Faculty of Engineering, King Mongkut's University of Technology Thonburi (KMUTT) for supporting this study.

Nomenclatures

A	area, m^2
A_{min}	minimum free flow area, m^2
A_f	surface area of fin, m^2
A_o	total surface area, m^2
A_p	cross-sectional or profile area of fin, m^2
Al	aluminium material
b	fin height, m
C_p	specific heat at constant pressure, J/(kg.K)
C^*	capacity rate ratio, dimensionless
C_c	cold-fuid capacity rate, W/K
C_h	hot-fluid capacity rate, W/K
Cu	copper material

d_f	outside diameter of finned tube, m
d_i	tube inside diameter, m
d_o	tube outside diameter, m
f	Fanning friction factor
f_b	fin base thickness, m
f_p	fin pitch, m
f_t	fin thickness, m
G_c	mass flux of the air based on minimum free flow area, kg/m^2.s
HX	heat exchanger
h	heat transfer coefficient, W/(m^2.K)
$I_{-1/3}$	modified Bessel function solution of the first kind, order -1/3
I_0	modified Bessel function solution of the first kind, order 0
$I_{2/3}$	modified Bessel function solution of the first kind, order 2/3
I_1	modified Bessel function solution of the first kind, order 1
j	Colburn factor
k	thermal conductivity, W/(m.K)
K_0	modified Bessel function solution of the second kind, order 0
K_1	modified Bessel function solution of the second kind, order 1
L	Length, m
m	mass flow rate, kg/s; fin performance parameter, m^{-1}
N_{row}	number of tube rows
NTU	number of transfer units, dimensionless
Nu	Nusselt number
P_L	longitudinal tube pitch, m
Pr	Prandtl number
P_T	transverse tube pitch, m
ΔP	pressure drop, Pa
Q	heat transfer rate, W
r_o	radius of tip fin, m
r_i	radius of base fin, m
R	radius function in terms of the radius ratio, dimensionless
Re_{di}	Reynolds number based on tube inside diameter
Re_{do}	Reynolds number based on tube outside diameter
T	temperature, ^{o}C
T_a	air temperature, ^{o}C
T_w	water temperature, ^{o}C
U	overall heat transfer coefficient, W/(m^2.K)
V_{fr}	frontal velocity, m/s
V_{max}	maximum velocity across heat exchanger,m/s

Greek symbols

ε	heat exchanger effectiveness
η	fin efficiency
η_o	overall surface effectiveness
ρ	density, kg/m^3
σ	contraction ratio of cross-sectional area
μ	dynamic viscosity of air, Pa.s
ϕ	combination of terms, dimensionless;
ψ	radius ratio

Subscripts

1	air-side inlet
2	air-side outlet
a	air
ave	average
b	base
c	cold fluid
f	fin
h	hot fluid
i	tube-side
in	inlet
m	mean value
max	maximum
o	air-side
out	outlet
t	tube
w	water

References

[1] P. Naphon and S. Wongwises, "Investigation of the performance of a spiral-coil finned tube heat exchanger under dehumidifying conditions," *J. Eng. Phys. Thermophys.,* Vol.76, pp.83-92, 2003.

[2] S. Wongwises and P. Naphon, "Heat transfer characteristics of a spiral-coil finned tube heat exchanger under dry-surface conditions," *Heat Transfer Eng*., Vol.27, pp.25-34, 2006.

[3] S. Wongwises and P. Naphon, "Thermal performance of a spiral-coil finned tube heat exchanger under wet-surface conditions," *J. Mech. Sci. Technol.,* Vol.20, pp.212-226, 2006.

[4] A. Nuntaphan, T. Kiatsiriroat and C.C. Wang, "Air side performance at low Reynolds number of cross-flow heat exchanger using crimped spiral fins," *Int Communications in Heat and Mass Transfer,* Vol.32, pp.151-165, 2005.

[5] A. Nuntaphan, T. Kiatsiriroat and C.C. Wang, "Heat transfer and friction characteristics of crimped spiral finned heat exchanger with dehumidification," *Applied Thermal Engineering*, Vol.25, pp.327-340, 2005.

[6] P. Pongsoi, S. Pikulkajorn and S. "Wongwises, Heat Transfer and Flow Characteristics of Spiral Fin-and-Tube Heat Exchangers: A Review," *Int. Journal of Heat and Mass Transfer,* Vol.79, pp.417-431, 2014.

[7] P. Pongsoi, S. Pikulkajorn, C.C. Wang and S. Wongwises, "Effect of fin pitches on the air-side performance of crimped spiral fin-and-tube heat exchangers with a multipass parallel and counter cross-flow configuration," *Int. Journal of Heat and Mass Transfer*, Vol.54, no.9-10, pp.2234-2240, 2011.

[8] P. Pongsoi, S. Pikulkajorn, C.C. Wang and S. Wongwises, "Effect of number of tube rows on the airside performance of crimped spiral fin-and-tube heat exchangers with a multipass parallel andcounter cross-flow configuration," *Int. Journal of Heat and Mass Transfer,* Vol.55, no.4, pp. 1403-1411, 2012.

[9] P. Pongsoi, S. Pikulkajorn and S. Wongwises, "Effect of fin pitches on the optimum heat transfer performance of crimped spiral fin-and-tube heat exchangers," *Int. Journal of Heat and Mass Transfer,* Vol.55, no.23-24, pp.6555-6566, 2012.

[10] P. Pongsoi, S. Pikulkajorn and S. Wongwises, "Experimental study on the air-side performance of a Multipass parallel and counter cross-flow L-footed spiral fin-and-tube heat exchanger," *Heat Transfer Engineering,* Vol.33, no.15, pp.1251-1263, 2012.

[11] P. Pongsoi, P. Promoppatum, S. Pikulkajorn and S. Wongwises, "Effect of fin pitches on the air-side performance of L-footed spiral fin-and-tube heat exchangers," *Int. Journal of Heat and Mass Transfer,* Vol.59, pp.75-82, 2013.

[12] P. Pongsoi and S. Wongwises, "Determination of fin pitches for maximum performance index of L-footed spiral fin-and-tube heat exchangers," *Journal of Thermal Engineering,* Vol.1, no.1, pp.251-261, 2015.

[13] P. Kiatpachai, S. Pikulkajorn and S. Wongwises, "Air-Side Performance of Serrated Welded Spiral Fin-and-Tube Heat Exchangers," *International journal of heat and mass transfer,* Vol.89, pp. 724-732, 2015.

[14] E.M.A. Mokheimer, "Performance of annular fins with different profiles subject to variable heat transfer coefficient," *Int. J. Heat and Mass Transfer,* Vol.45, pp.3631-3642, 2002.

[15] E.M.A. Mokheimer, "Heat transfer from extended surface subject to variable heat transfer coefficient," *Heat and Mass Transfer,* Vol.39, pp.131-138, 2003.

[16] D.E. Briggs and E.H. Young, "Convective heat transfer and pressure drop of air flowingacross triangular pitch banks of finned tubes," *Chem. Eng. Prog. Symp Ser.,* Vol.59, no.41, pp.1–10, 1963.

[17] C.C. Wang and C.T. Chang, "Heat and mass transfer for plate fin-and-tube heat exchangers with and without hydrophilic coating," *Int. J. Heat Mass Transfer*, Vol.41, pp.3109–3120, 1998.

[18] C.C. Wang, Y.J. Chang, Y.C. Hsieh and Y.T. Lin, "Sensible heat and friction characteristics of plate fin-and-tube heat exchangers having plane fins," *Int. J. Refrig.,* Vol.19, no.4, pp.223–230, 1996.

[19] V. Gnielinski, "New eguation for heat and mass transfer in turbulent pipe and channel flow," *Int. Chem. Eng.,* Vol.16, pp.359–368, 1976.

[20] K.A. Gardner, "Efficient of Extended Surface, ASME Trans.", Vol.67, pp.621, 1945.

[21] W.M. Kays, A. London, Compact heat exchangers, 3rd Ed., Mcgraw-Hill, New York, 1984.

[22] Y.G. Park, "Correcting energy balance error in heat exchanger data by maximum likelihood method," *Applied Thermal Engineering*, Vol. 131, pp.311–319, 2018.

[23] S. Kakac, H. Liu and A.Pramuanjaroenkij, Heat Exchangers: Selection, Rating and Thermal Design, 3rd ed. Boca Raton, FL: CRC Press. Kakaç, S., 2012.

Author's history:

Dr. Parinya Kiatpachai is a lecturer of mechanical engineering at Department of Mechanical Engineering, Academic Division, Chulachomklao Royal Military Academy (CRMA). He received his D.Eng. in mechanical engineering from the King Mongkut's University of Technology, Thonburi, Bangmod, Thailand. His current research interests include the heat transfer performance and flow characteristics of fin-and-tube heat exchangers.

Asst.Prof.Dr. Anotai Suksangpanomrung is a assistant professor and head of mechanical engineering at Department of Mechanical Engineering, Academic Division, Chulachomklao Royal Military Academy (CRMA).

Mr. Phubate Thiangtham is a MD & Project Manager at Thai-Ingenieur Co., Ltd. He received his M.Eng. in mechanical engineering from the King Mongkut's University of Technology, Thonburi, Bangmod, Thailand.

Mr. Chanyoot Keepaiboon is a MD & Project Manager at Thai-Ingenieur Co., Ltd. He received his M.Eng. in mechanical engineering from the King Mongkut's University of Technology, Thonburi, Bangmod, Thailand.

Assoc.Prof.Dr. Weerapun Duangthongsuk is a associate professor of mechanical engineering at Department of Mechanical Engineering, Southeast Asia University (SAU). His research interests include heat transfer, fluid mechanics, and nano fluids.

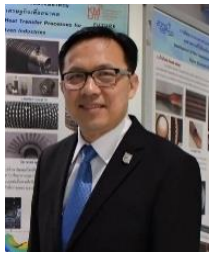

Prof.Dr. Somchai Wongwises is a professor of mechanical engineering at King Mongkut's University of Technology, Thonburi, Bangmod, Thailand. He received his Doktor-Ingenieur (Dr.-Ing.) in mechanical engineering from the University of Hannover, Germany, in 1994. His research interests include two-phase flow, heat transfer enhancement, and thermal system design. He is the head of the Fluid Mechanics, Thermal Engineering and Multiphase Flow Research Laboratory (FUTURE).